ARTICLE NO. 78-1454R

Fuel Consumption of a Strutted vs Cantilever-Winged Short-Haul Transport with Aeroelastic Considerations

Paul H. Park*
General Dynamics Corporation, Fort Worth, Texas

A preliminary design of a short-haul aircraft using a strut-braced wing was made to study the possibility of block fuel savings caused by the decrease in wing weight allowed by the use of a strut. A computer-aided wing loads and stress analysis was performed to determine the wing weight savings. It was found that the wing weight savings are not large in this aircraft and the induced drag decrease is offset by the strut parasite drag. The final cantilever and strutted configurations have essentially equal block fuel consumptions. A calculated strut flutter velocity was close enough to the flight envelope to warrant design consideration.

Nomenclature

a	= coordinate of strut-wing juncture, ft
A_M	= modal magnitude of strut angular twist, rad
AR	= aspect ratio
b	= wing span, ft
c	= chord, ft
C_3, C_4	= integration constants
E	= elastic modulus, psi
$( )g$	= loading equaling ( ) times the aircraft's weight
G	= shear modulus, psi
h	= normal displacement of strut measured from the elastic axis, ft
H	= altitude, ft
H_N	= modal magnitude of strut displacement
$I, I(y)$	= material area moment of inertia, in.^{4}
J	= material polar area moment of inertia, in.^{4}
l	= length, ft
M	= mode index
MAC	= mean aerodynamic chord, ft
M_C	= Mach number at V_C
$M(y)$	= wing bending moment, lb-ft
N	= mode index
OWE	= operating weight empty (includes crew), lb
P	= strut tension = S_t, lb
$p, p(y)$	= wing spanwise loading (aerodynamic plus dead weight), lb/ft
S	= wing reference planform area, ft^2
S_c	= horizontal component of strut tension, lb
S_t	= strut tension = P, lb
S_W	= vertical component of strut tension, lb
t	= time
t/c	= thickness to chord ratio
TOW	= takeoff weight, lb
V_A, V_B, V_C, V_D	= FAR part 25, flight loading envelope reference velocities, knots
V_e	= equivalent velocity, knots
V_{S_1}	= stall speed with airplane in cruise configuration, knots
$\bar{V}$	= tail volume ratio
w	= vertical displacement of a point on the wing chord plane, ft
$W(y), W_{st}(y)$	= see Eqs. (3a and 3b)
y, Y'	= spanwise coordinate, ft
ZFW	= zero fuel weight, lb
α	= angle of twist, rad
γ	= climb gradient
$\theta(y), \theta_{st}(y)$	= see Eqs. (4a and b)
$\Lambda_{c/4}$	= quarter chord sweep angle
σ	= taper ratio
ω_H	= natural frequency of assumed bending mode
ω_α	= natural frequency of assumed torsion mode
$( )_{st}$	= value of ( ) for strut
$\langle y-a \rangle^{-1}$	= Dirac delta function at $y=a$

Presented as Paper 78-1454 at the AIAA Aircraft Systems and Technology Conference, Los Angeles, Calif., Aug. 21-23, 1978; submitted Sept. 4, 1979; revision received March 6, 1980.

Index categories: Performance; Structural Design; Aeroelasticity.

*Senior Design Engineer. Member AIAA.

Introduction

THE increased cost and potential decreased availability of hydrocarbon fuel in recent years has led to increased research in the aeronautical community for possible methods of developing more fuel-efficient aircraft.[1] Most of the effort has been directed toward large, high-speed aircraft serving high-density or long-range markets. The introduction of a highly fuel-efficient aircraft to the infamously money-losing short-haul or medium-density market, however, could significantly aid in the profitability of these routes.

Two important ways of increasing aircraft miles per gallon by decreasing drag are to increase the aircraft's aerodynamic efficiency and to decrease its weight. Increasing the aircraft's wing aspect ratio makes the wing a more efficient lifting device; however, high aspect ratios increase structural loads on wings, causing an increase in the aircraft's weight. If a strut is added to the aircraft's wing, much of the structural weight penalty of the higher aspect ratio wing can be removed. The ever-present tradeoff in this instance is the drag and weight increase due to the strut. The bulk of this paper is dedicated to whether or not this tradeoff will result in less total drag and less block fuel consumption for an aircraft designed for the short-haul medium-density market.

Design Method

The outline of the design procedure is as follows.

1) Establish initial configuration and calculate parasite drag of strutted aircraft.

2) Establish alternate configurations by changing wing areas.

3) Evaluate performance parameters of the configurations.

4) Perform a weight and range analysis to determine a first iteration mission size (takeoff weight and wing area) of the strutted aircraft assuming a cantilever wing weight.

5) For the mission configuration, determine the weight savings caused by the strut.

6) Do a refined weight and range analysis of both the strutted and cantilever aircraft.

Table 1 Mission definition

Type of aircraft	Short range, 80-passenger transport, two-engine turboprop
Typical mission	
Payload	18,000 lb total cargo and passengers
Cruise	300 mph at 25,000 ft
Range	Two 500-statute-mile stages, with adequate reserve
Takeoff	4500 ft
Landing	4500 ft

7) Determine and compare block fuel consumption.
8) Perform an aeroelastic analysis of the strut.

The design method used in steps 1-4 of the outline was based mainly on techniques described by Shevell,[2] with occasional use of Nicolai's design book.[3] Only the mission definition and the mission-sized configurations are described in this paper.

It must be emphasized that the mission configuration is a first iteration design, and its purpose was to provide an estimate of the wing size and geometry and the aircraft weights. These parameters were used to carry out the wing weight analysis of step 5.

The mission definition, including type of aircraft and typical mission, are given in Table 1.

Mission-Sized Configuration

The basic results of design steps 1-4 are shown in Figs. 1-5. Figure 1 shows the cabin layout with its five-abreast configuration. In an effort to create a cabin environment with comfort standards equivalent to contemporary narrow body transports, the seats were designed with a 17.9-in. width between armrests and a 35-in. seat pitch. The aisle is 20 in. wide, and the cabin height is 7 ft. Figure 2 is a three-view layout of the mission-sized aircraft. The engines are based on a new technology turboprop described in Ref. 4. Takeoff requirements sized the 16-ft-diam propeller and the 4830 sea level shaft horsepower (slshp) engine. The engines were placed 22 ft outboard of the centerline to achieve at least 5-dB noise reduction at the cabin side.[4] The main landing gear consists of two four-wheel bogies that retract into fuselage pods. The wing uses an airfoil similar to the NASA GA(W)-2 airfoil[5] and has t/c of 14%. The double-slotted flaps are 33% constant percentage chord. An initial strut configuration was designed to provide drag estimations. It used a symmetrical section with a t/c of 12%.

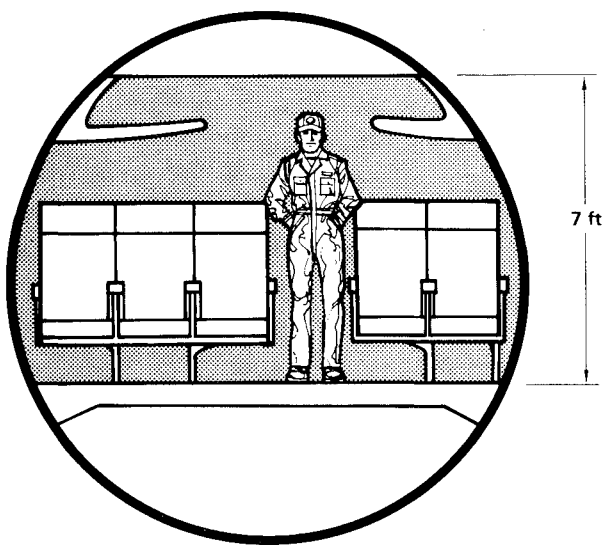

Fig. 1 Fuselage cross section.

The FAA speed and positive g gust and maneuver load envelopes are shown in Figs. 3 and 4. The zero fuel weight (ZFW) case was the critical load condition owing to the wing located fuel weight of only 13% of the takeoff weight. The 2.5-g maneuver load requirement is shown to be critical. The high altitude, low speed, and high wing loading combined to keep the gust loads relatively small.

Figure 5 is the mission-sizing performance summary chart. Landing, takeoff, second segment climb, and range performance are plotted vs takeoff weight and wing area. The mission configuration was chosen near the apex of the acceptable configuration region at a wing area of 764 ft^2 and takeoff weight of approximately 70,000 lb.

Wing Loads Analysis and Determination of Cantilever Structural Wing Box Weight

The wing loading for the critical loading condition was calculated using Schrenk's method. The critical loading was determined to be the 2.5 g maneuver load at V_c and 20,000 ft. A graph of the resulting semispan loading is shown in Fig. 6. The engine weight was distributed over 4 ft of span in absence of a structural arrangement of the wing-engine mounting. The curve of Fig. 6 was integrated twice to obtain the shear and moment distributions for the critical loading.

Given the spanwise distribution of shear and moment and the geometric characteristics of the wing box, the wing box

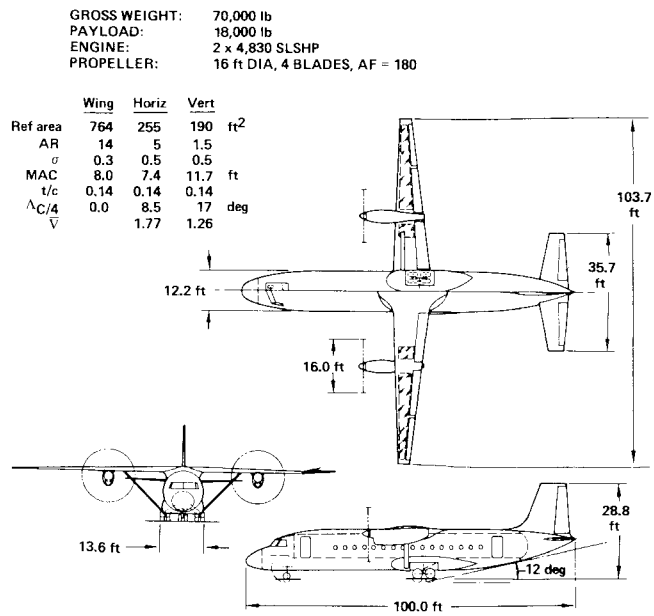

Fig. 2 General arrangement.

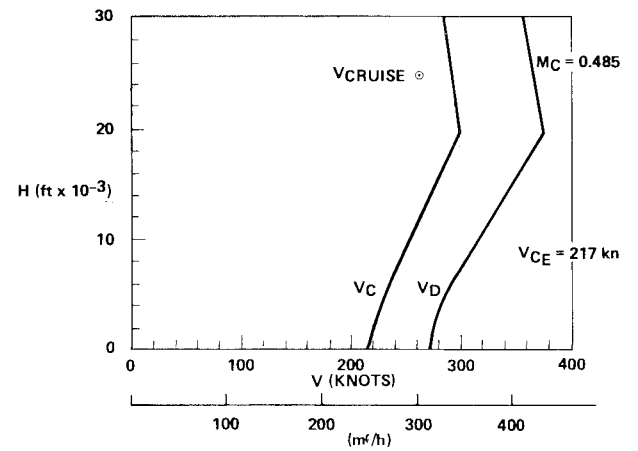

Fig. 3 Placard speeds.

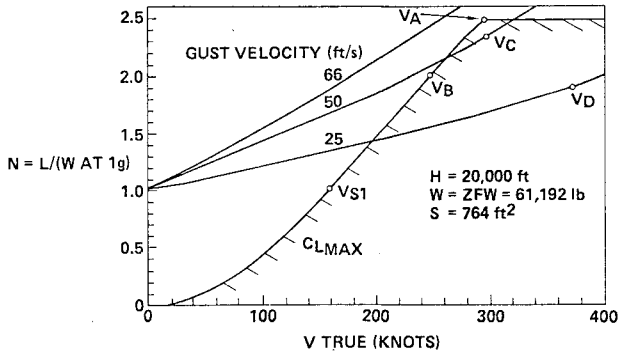

Fig. 4 Gust and maneuver loads.

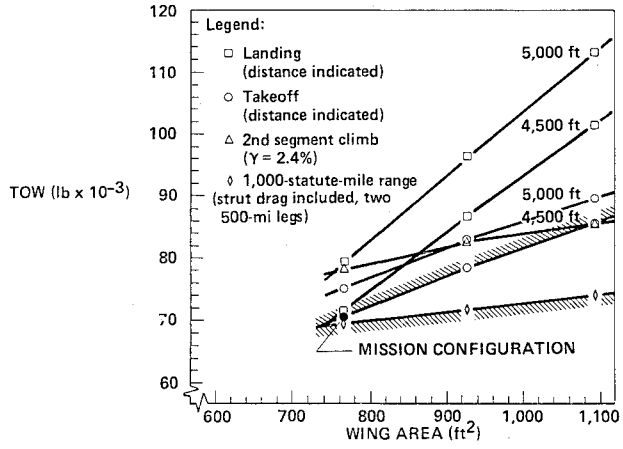

Fig. 5 Summary chart.

and stiffened skin material thicknesses were then determined. Material area as a function of span was calculated from the thicknesses. The plot is shown in Fig. 7. The curve was numerically integrated over the span, and the material volume and weight were determined. The resulting wing box weight, based on bending material only, was 2428 lb. This weight is only 29% of the total wing weight of 8365 lb, and only 5.6% of the operating empty weight of 43,194 lb.

Strutted Aircraft Wing Weight Analysis

The task of determining the amount of wing box weight that can be eliminated by use of a strut was accomplished using an iterative procedure that is a combination of a method for determining particular solutions to the beam bending equation of the wing and the method described in the previous section for determining wing box material areas and skin thicknesses.

Using Fig. 8, the method begins with the beam equation for the wing. Beam force equilibrium (force/length):

$$\frac{d^2}{dy^2}\left(EI(y)\frac{d^2w}{dy^2}\right)=p(y)-S_w\langle y-a\rangle^{-1} \tag{1}$$

$\langle\ \rangle^{-1}$ is the Dirac delta function.

Integrating Eq. (1) four times produces the equation for wing deflection

$$w=W(y)-S_wW_{st}(y)=C_3y+C_4 \tag{2}$$

where

$$W(y)=\int_0^y\theta(\xi)d\xi \tag{3a}$$

$$W_{st}(y)=\int_a^y\theta_{st}(\xi)d\xi \tag{3b}$$

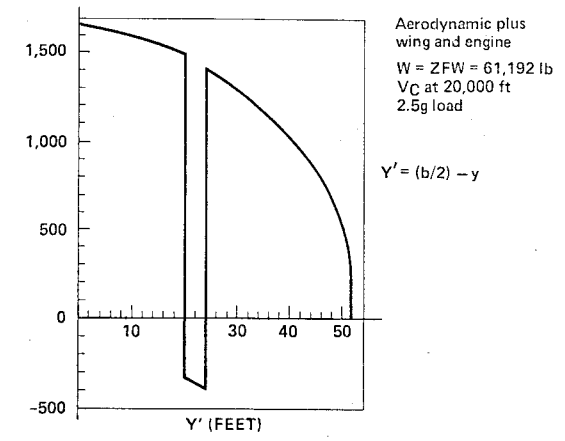

Fig. 6 Wing loading, critical case.

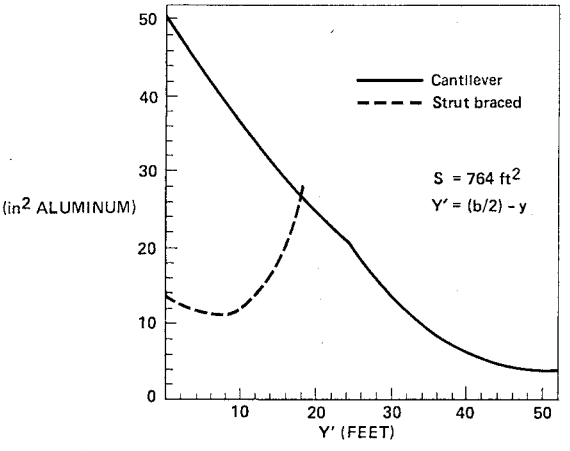

Fig. 7 Wing structural box material cross-sectional area.

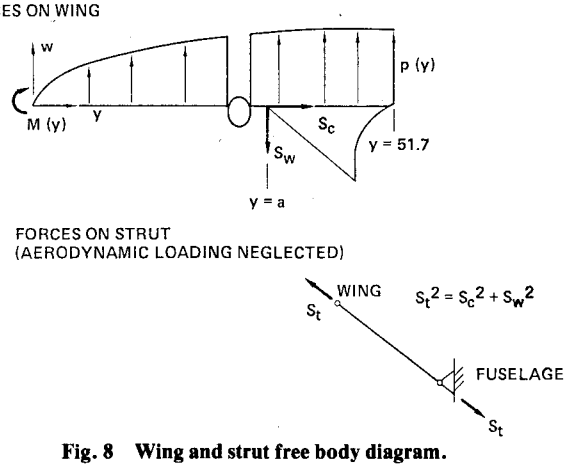

Fig. 8 Wing and strut free body diagram.

$$\theta(y)=\int_0^y\frac{M(\xi)}{EI(\xi)}d\xi \tag{4a}$$

$$\theta_{st}(y)=\int_a^y\frac{(\xi-a)}{EI(\xi)}d\xi \tag{4b}$$

$\theta(y)$, $\theta_{st}(y)$, $W(y)$ and $W_{st}(y)$ are calculated by numerical integration based on the known $M(y)$ distribution and an assumed $I(y)$ distribution. The unknowns S_w, C_3 and C_4 are determined from the following boundary conditions:

at $y=5.17$ ft (wing root)

$$w=0=W(51.7)-S_wW_{st}(51.7)+[C_3x51.7]+C_4 \tag{5a}$$

$$\frac{dw}{dy} = 0 = \theta(51.7) - S_w\theta_{st}(51.7) + C_3 \qquad (5b)$$

at $y = a$ (strut juncture)

$$w = \frac{S_w l_{st}}{A_{st}E_{st}} = W(a) + [C_3 xa] = C_4 \qquad (6)$$

where l_{st} is the strut length, E_{st} the strut elastic modulus, and A_{st} the strut material cross-sectional area.

Solving Eqs. (5a, 5b, and 6) for S_w

$$S_w = \frac{w(31.7) + [51.7-a]\theta(51.7) - W(51.7)}{(l_{st}/E_{st}A_{st}) + [51.7-a]\theta_{st}(51.7) - W_{st}(51.7)} \qquad (7)$$

The assumption is made that the first term in the denominator of Eq. (7) is small with respect to the other terms in the denominator and can be neglected. Physically this assumption means that the wing deflection at the strut juncture would be small and would not affect the value of the load carried by the strut. The assumption is applied by setting the left-hand side of Eq. (6) equal to zero. Later results confirmed the assumption's validity. Values of $(l_{st}/E_{st}A_{st})$ were less than 1% of the value of the rest of the denominator in all cases.

With S_w known, the moment and shear distributions between the root and strut juncture can be calculated. Required skin thicknesses and resulting material areas and area moment of inertias are then determined. Since a free-ended pinned bar can support only loads applied along its axis, the strut applies a direct compression load on the wing S_c, as well as the down load, S_w (Fig. 8). This compression load is included in evaluating the compression and tension loads on the wing box airfoil skins.

A computer program was written that numerically evaluated $M(y)$, $\theta(y)$, $\theta_{st}(y)$, and $W_{st}(y)$. The program used a simple trapezoidal algorithm to perform the integrations. The program inputs were the shear distribution, the elastic modulus of the wing, and an assumed moment of inertia distribution that is iterated upon. The program's output was used to evaluate S_w, C_3, and C_4 using Eqs. (5a,b, and 6).

The method was applied to two different length struts for the zero fuel weight (ZFW) critical load condition. The first strut was 18.4 ft long and was attached to the wing 20 ft out from the root ($a = 31.7$ ft). The second strut was 17 ft long and was attached to the wing 18 ft out from the root ($a = 33.7$ ft). The initially assumed $I(y)$ distribution was calculated assuming use of minimum skin gage thickness (0.06 in.) for the structural box between the root chord and the strut juncture. The cantilever wing $I(y)$ distribution was used for wing positions outboard of the strut juncture in all iterations. The $I(y)$ distribution was iterated until calculated S_w values converged to a difference of less than 5%.

Figure 9 shows the convergence of the moment of inertia distributions between the root chord and the strut juncture for the 17-ft strut. For the 2.5-g loading, strut tensions S_t of 111,890 lb resulted for the 18.4-ft strut, and 117,788 lb resulted for the 17-ft strut.

The wing box material area distributions for the two struted wings were calculated and integrated to determine the material volume and weight of the wing box. The wing box material area vs span for the 17-ft strut configuration is shown in Fig. 7. Total structural box weights (not including the strut) of 1493 lb resulted for the 18.4-ft strut, and 1600 lb resulted for the 17-ft strut. These values show a 39% and 34% reduction in structural box weight, but only a 2.2% and 1.9% decrease in operating weight empty.

FAA regulations also require the aircraft to sustain a $-1g$ maneuver load; therefore, a loads analysis was done for the two strutted wings to determine the maximum compression loads applied to the struts and to see that the wing box material needed to support a $+2.5g$ load also was distributed properly enough to support a $-1g$ load. Schrenk's method was used to calculate the loading, and the final $I(y)$ distributions for the strutted wings was input. The check showed that the thicknesses were adequate. A total strut compressive load S_t of 49,128 lb was calculated for the 18.4-ft strut and a 51,605 lb load was calculated for the 17-ft strut.

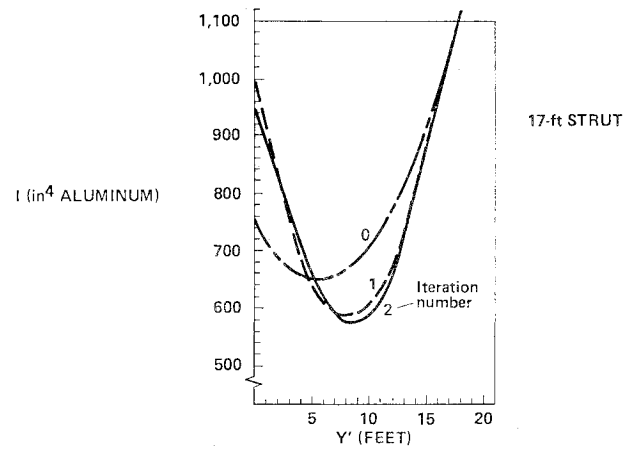

Fig. 9 Structural box area moment of inertia iterations.

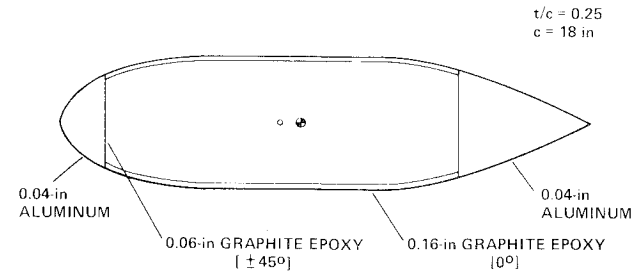

Fig. 10 Strut cross section.

Strut Design

Given the $-1g$ strut compressive loading, a more detailed design of the strut was done. The high loads caused the original strut design to be woefully inadequate in buckling resistance. In order to provide a 1.5 buckling safety factor for the strut, the strut was redesigned with a t/c twice that of the initial design. Graphite epoxy was used to provide the proper stiffness at an adequate weight. This cross section used on the 17-ft strut gave a 1.54 safety factor. The 17-ft length was chosen, and the estimated weight of the two struts was 121 lb. The thicker strut caused a 25% increase in strut parasite drag. Figure 10 shows the strut cross section.

Block Fuel Consumption Comparison

The bottom line task of the design was to redo the weight-range analysis for both the strutted and cantilever configurations. Total parasite drags were recalculated based on the new strut design. The strutted aircraft had a total aircraft parasite drag coefficient of 0.0261, a 4% increase over the cantilever aircraft. The weight analysis used a statistical computer program, which was modified for the strutted aircraft by applying a factor of 0.911 to the wing structural weight. This factor is the ratio of the total strutted wing weight to the cantilever wing weight for the 70,000 lb aircraft. Table 2 lists the results. The 51-lb difference in fuel con-

Table 2 Weights of the final aircraft configurations[a]

Type	TOW, lb	OWE, lb	Fuel weight, lb
Cantilever	70,420	43,349	9071
Strutted	69,778	42,656	9122

[a] Range, 1000 mi.; payload, 18,000 lb.

sumption is well within error range of the analysis, and a conclusion of essentially equal block fuel consumptions for the two aircraft was made.

Aeroelastic Analysis of the 17-ft Strut

The use of a 17-ft-long strut in equivalent airspeeds of up to 459 ft/s (Fig. 3) makes flutter a hazard that must be given design consideration. The fact that destructive strut flutter can occur was amply demonstrated by the loss of the model I Israeli Arava aircraft during flight test.[6]

In this analysis the two-dimensional, incompressible, unsteady aerodynamics of Theodorsen[7] and one-dimensional beam-type structural dynamics were used. The Laplace transformation in time was performed on the equations of motion instead of the classic assumption of simple harmonic motion. Aerodynamic forces in the transformed domain were calculated using the generalized Theodorsen function as described by Edwards.[8] Root locus plots of the stability determinant were made to determine the outset and severity of instabilities.

The force and moment equations were derived based on the typical section approach of Bisplinghoff, Ashley, and Halfman.[9] Deflection h and angular twist a were expressed as functions of time t and strut span y. The torsional spring in Ref. 11 is replaced by $GJ[\partial^2\alpha(y,t)/\partial y^2]$. The displacement spring is replaced by

$$EI\frac{\partial^4 h}{\partial y^4}(y,t)+P\frac{\partial^2 h}{\partial y^2}(y,t)$$

P is the axial force on the strut. Sinusoidal spanwise bending and torsion modes were assumed, and Galerkin's method was applied to the Laplace-transformed equations to obtain a stability determinant. The determinant was expanded for two and three assumed modes (one bending, one torsion; two bending, one torsion).

The resulting equation is a function of the modal integers, the Laplace transform variable p and velocity. For a given mode combination, root locus plots of p were developed using velocity as the gain parameter. The plots were developed using an iterative computer program which solved the characteristic equation for p (Ref. 4). Flutter was evidenced by the crossing of the locus into the positive real quadrants.

One mode combination grew unstable near the velocity range of the flight envelope. It occurred for the first bending and "one-half" torsion mode. This torsion mode of a half sine wave simulated a wing strut juncture of zero torsional stiffness. Since wing strut junctures are usually made with a single fitting, this is a conservative but not unreasonable assumption. This merging frequency-type vibration goes unstable at 680 ft/s, only 8% over V_D. Figure 11 shows the root locus plot. The second pair of loci are the plots of the same first bending, one-half torsion roots that result when three modes are assumed. (The second bending root is stable and not shown.) The shapes of the two pairs are quite similar.

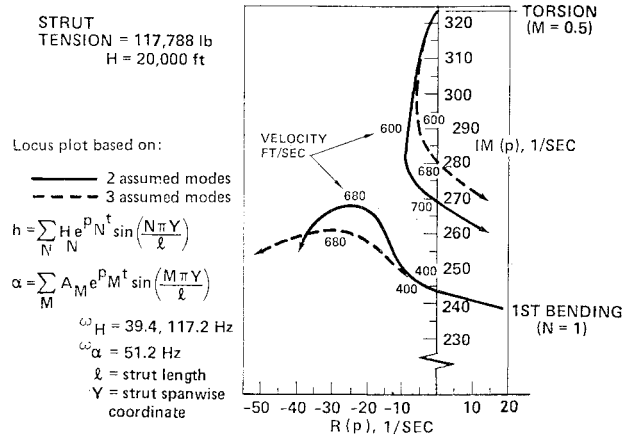

Fig. 11 Root loci for $N=1$, $M=0.5$ assumed modes.

Summary

Several factors combined to prevent the strut from accomplishing its intended purpose. The critical load factor for the airplane was low, and the modern technology highly loaded wing kept the span and resulting moment arms small. This produced a cantilever wing whose structural box weight was only 5.6% of the aircraft's operating weight empty (includes crew) (OWE). The 30% savings in the structural wing box weight allowed by use of the strut resulted in only a 1.6% decrease in OWE. Finally the larger than anticipated strut t/c ratio increased the original strut drag estimates. Therefore, a strutted wing does not appear practical for this type of transport category aircraft.

The strut flutter analysis shows that design consideration must be given to the strut wing juncture to insure high enough torsional stiffness to force higher torsional vibration modes.

Acknowledgments

The author wishes to thank his two advisors at Stanford University, H. Ashley and R. Shevell, for their help and patience.

This research was sponsored by NASA Grant NGL-05-020-243.

References

[1] Provinelli, F.P., Klinberg, J.M., and Kramer, J.J., "Improving Aircraft Energy Efficiency," *Astronautics & Aeronautics,* Vol. 14, Feb. 1976, pp. 18-31.

[2] Shevell, R.S., "Introduction to Aerospace Systems Synthesis and Analysis," Stanford University Dept. of Aeronautics and Astronautics, copies available from the author.

[3] Nicolai, M., "Fundamentals of Aircraft Design," School of Engineering, University of Dayton, Dayton, Ohio, 1975.

[4] "Study of Operational Requirements for Medium Density Air Transportation," Douglas Aircraft Co., Summary: Volume I, NASA CR-137603, 1974.

[5] McGhee, R.J., Beasley, W.D., and Somers, D.M., "Low Speed Aerodynamic Characteristics of a 13-Percent-Thick Airfoil Section Designed for General Aviation Applications," NASA TM X-72697, May 1975.

[6] Coleman, H.J., "Arava Performs Well in STOL Mode," *Aviation Week and Space Technology,* Vol. 94, June 1971, pp. 54-57.

[7] Theodorsen, T., "General Theory of Aerodynamic Instability and the Mechanism of Flutter," NACA Rept. 496, 1935.

[8] Edwards, J.W., "Unsteady Aerodynamic Modeling and Active Aeroelastic Control," Stanford University Department of Aeronautics and Astronautics Rept. 504, Stanford, Calif., Feb. 1977.

[9] Bisplinghoff, R.L., Ashley, H., and Halfman, R.L., *Aeroelasticity,* Addison-Wesley Publishing Co., Reading, Mass., 1955.